JOURNAL OF THERMOPHYSICS AND HEAT TRANSFER
Vol. 25, No. 1, January–March 2011

Influence of Solution Hydrodynamics on the Deposition of $CaSO_4$ Scale on Aluminum

Abdul Quddus* and Luai M. Al-Hadrami†
King Fahd University of Petroleum and Minerals, Dhahran 31261, Saudi Arabia

DOI: 10.2514/1.44865

The dissolution of hard and adherent scaling species depositing from process fluid streams is a serious problem experienced by the world's processing and petrochemical industries. Scaling/fouling causes a significant economic loss. Scaling is a complex process; therefore, this laboratory study employed a rotating cylinder electrode apparatus to develop a basic understanding of the scaling phenomenon. The effect of solution hydrodynamics was investigated at various rotational speeds on the deposition of calcium sulfate ($CaSO_4$) scale on aluminum substrate having surface roughness profiles produced with 120 and 600 grit silicon carbide emery papers and at temperatures of 60 and 70°C. The results indicate a strong impact of solution hydrodynamics on the deposition rate of calcium sulfate on aluminum specimens. Morphological examinations of the deposited scale crystals under scanning electron microscope and energy dispersive *X*-ray spectrometry revealed prismatic needles and rodlike crystals growth at nucleation sites branching out randomly over the substrate. Secondary growth on the already existing primary crystals of $CaSO_4$ was also discerned.

Nomenclature

D_r	=	deposition rate of scale ($g.m^{-2}.h^{-1}$)
L	=	length of specimen, cm
R_a	=	average surface roughness, μ inch
Re	=	equivalent Reynolds number
R_1	=	radius of specimen, cm
R_2	=	inner radius of glass cell, cm
s	=	solid phase formation due to precipitation
t	=	time, h
$U_{c,Re}$	=	uncertainty in Reynolds number, %
$U_{c,Dr}$	=	uncertainty in deposition rate, %
υ	=	kinematics viscosity, cm^2/s
W_g	=	weight gain of specimen due to scale, g
μ	=	micro (10^{-6})
ω	=	angular velocity of specimen, rad/s
aq	=	aqueous
1 μ inch	=	0.0254 μm

I. Introduction

THE insoluble, hard, and adherent inorganic mineral substances depositing from process fluid streams onto the hot surface(s) is termed scaling or fouling. These superfluous deposits pose major problems for the process industries worldwide because of unpredictable failures and frequent shutdowns caused by scaling. This is a precarious situation and a safety hazard, which sometimes causes fatal accidents attributed to complete choking of the piping system(s), in addition to economic penalties. The scale deposits on heat transfer surfaces badly reduce the thermal efficiency of heat transfer equipment. Because of the adherent and mechanically resilient solid scale, reduction in fluid flow, localized heating and pressure gradients occur in the piping systems of the process plants which in turn demand additional pumping power. The plants thus incur an extra operational cost. In heat exchangers, deposits of scale on the tubes substantially reduce their ability to exchange heat effectively. In desalination plants, the scale deposits affect both the quality and quantity of produced potable water. Scale deposits comprising mainly alkaline earth sulfates and carbonates are usually found in oil producing wells; these restrict flow through the tubings and hence reduce oil production. Thus, decrease in thermal efficiency and/or reduction of flow rate results in decline of revenues [1,2]. The synergistic effect of scale and corrosion, moreover, is an important problem that plant designers and operators have to battle with throughout the useful service life of a plant [3].

The basic understanding of scale formation is therefore essential for an effective control and scale mitigation program. Scale formation is a complex process, which involves many factors such as: adequate solution supersaturation, temperature, pressure, hydrodynamic conditions of fluid flow systems, etc. Flow dynamics may play an important role in the scale formation process among these factors; therefore, this study has explored hydrodynamics effects. Thus, a research program was initiated to understand the deposition of minerals scales on commercial grade metallic materials. Commercial grade aluminum was selected for the study because it is one of the construction metals used commonly in industry, either in pure or alloyed form.

To study scale deposition in the laboratory, commonly, two methods are practiced: 1) static bench experiments called beaker tests [2,4], and 2) dynamic open- or closed-loop tests [2,5–9]. In static tests, samples of two incompatible waters or scale-forming solutions are commingled together and the weight of precipitation measured gravimetrically after an interval of time. The mixed solutions can remain quiescent, hand shaken or being stirred during the test interval, and if desired seeded growth of crystallization can also be achieved [2,4]. In certain cases, the results of the tests can also be corroborated by employing: 1) analytical/chemical methods that can determine the amount of precipitation expected from the given blend of two solutions of known composition, temperature, and pH, etc, [2,4], and 2) dynamic experiments [2,5–9], involving open- (once through type) or closed-flow loops (recirculating type). Static experiments are useful for laboratory screening purposes but have limitations. Flow loop experiments, on the other hand, are representative of practical situations encountered in industry but are laborious and time consuming usually requiring extended periods of rigorous monitoring along with copious volumes of feed solution.

Alternatively, it is relatively easy to use rotating cylinder electrode (RCE) or rotating disk electrode (RDE) to study scale formation in the laboratory. The RDE and RCE techniques are well-established methods for studying kinetics of corrosion [10–14] and electrodeposition [15,16]. These techniques have also been used for the study of scale deposition to a limited extent [17–23].

Received 10 April 2009; revision received 8 December 2009; accepted for publication 13 December 2009.

*Research Institute, P.O. Box 1524; amquddus@kfupm.edu.sa.
†Research Institute, P.O. Box 1207; luaimalh@kfupm.edu.sa.

We selected RCE for our experimental study, as compared with RDE, primarily because of its analogy to the pipe surface geometry, and secondly because the cylindrical surface provides more surface area than a round flat disk. These features were considered advantageous for our work. No attempt was made to explore the electrochemical aspects in the present work. Therefore, we obtained the scale deposition results on aluminum substrate having two surface roughness profiles under different hydrodynamic conditions (i.e., at various rotational speeds) at 60 and 70°C. The selected temperature range for the study is representative of the operating temperatures being used in most of the process industries in the Gulf region.

Neville et al. [19,20] and Neville and Morizot [21] studied the deposition of $CaCO_3$ on a rotating disk electrode surface made from SS-316L at different rotational speeds. They used a well-known oxygen reduction electrochemical technique in their study. With the oxygen reduction process, they were able to show that the coverage of sample surface with scale resulted in the reduction of electroactive surface area and the corresponding electrochemical response. They demonstrated that the surface coverage predicted by their proposed electrochemical technique and that of image analysis conducted on the surface of scaled and clean samples supported each other. The technique is helpful in understanding the scale formation, assessment of inhibitors and their adsorption on the solid surface.

Morizot et al. [22] employing the electrochemical technique developed by Neville et al. [19], further studied the inhibition of $CaCO_3$ scale on an SS-316 rotating disc electrode surface by varying the dosage of polyacrylic acid (PAA), a proprietary scale control inhibitor intended for use to inhibit both the bulk precipitation as well as scale formation on the metal surface. They evaluated the effectiveness of the PAA-inhibitor by applying the above stated electrochemical technique and showed that the efficiency of the inhibitors may be quite varying in relation to the surface deposition and bulk precipitation in the scaling solution.

Chen et al. [23] studied the $CaCO_3$ scale formation on a rotating disk electrode surface in three different supersaturated scale-forming solutions by using the technique proposed by Neville et al. [19]. They showed that scale deposition on the surface of the specimen and the precipitation in bulk of solution are different processes, which depend on the indices of supersaturation of the solutions. They monitored the surface coverage of the RDE with the scaling by oxygen reduction electrochemical phenomenon at the RDE surface under potentiostatic control, which showed that the presence of scale on the samples resulted in the reduction of electrical current with time during their experiments.

Singh and Abbas [24] conducted laboratory characterization and analyses on the actual scale samples that were obtained from the choked oil production pipelines from the oil fields of the Arabian Gulf region. They found that the calcium sulfate, strontium sulfate, barium sulfate, and calcium carbonate are the most commonly formed scales in the Arabian Gulf.

In the earlier work [18,19], the deposition of barium sulfate and calcium sulfate scales on SS-316 surface was studied at various rotational speeds by using rotating cylinder electrode equipment. The present paper reports the results of calcium sulfate scale that was hydrodynamically deposited by using RCE technique on the commercial grade aluminum available in the market.

II. Experimental

The cylindrical test specimens of 1.27 cm long and 1.27 cm in diameter having a central hole were machined from commercial grade aluminum rod. Samples were fitted on to the shaft of the RCE equipment so that only the peripheral surface was exposed to the scale-forming solution.

The schematic of an EG&G Princeton Applied Research Rotating Cylinder Electrode test setup is shown in Fig. 1. The full detail of experimental test setup including improvised glass test cell used in the study can be found elsewhere [17,18].

Analytical grade anhydrous reagents: $CaCl_2$ and Na_2SO_4 were dissolved in deionized water to produce $CaSO_4$ by coprecipitation.

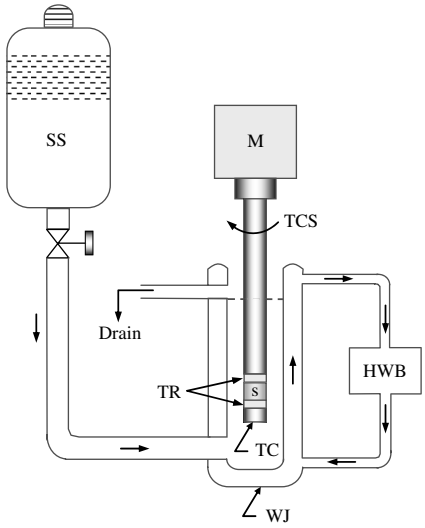

M = MOTOR TO ROTATE SPECIMEN AT FIXED RPM
TCS = TEFLON COATED SHAFT.
TR = TEFLON RING
S = CYLINDRICAL SPECIMEN
TC = TEFLON CAP
HWB = HOT WATER CIRCULATION BATH
SS = SUPERSATURATED SOLUTION
WJ = WATER JACKET
WCB = HOT WATER CIRCULATION BATH

Fig. 1 Schematic of the experimental setup of RCE equipment.

Concentration of each salt was kept at 0.03 mole/liter. Equal volumes of the two equimolar solutions were mixed in a translucent reservoir connected to the rotating cylinder's glass cell. A single pass flow arrangement was made whereby the replenishment of supersaturated solution to the test cell was kept around 1 to 1.5 liter/h. The flow of the scale-forming solution to the cell was accomplished by gravity. This arrangement facilitated the exposure of specimens to a solution of constant composition throughout the experimental run. We used pure laboratory grade chemicals, therefore, no filtration of the solution(s) was considered necessary. The experiments were conducted for two surface roughness profiles produced by 120 and 600 grit silicon carbide (SiC) emery papers, at 60 and 70°C, respectively. The experiments were conducted at atmospheric pressure for 6 h duration at various selected rotational speeds up to 2000 rpm (rpm). After polishing the samples were degreased with acetone, rinsed with distilled water and dried by compressed clean air. At least a minimum of triplicate experiments were performed at each preset rotational speed and outlier points if any, further repeated. The average scale deposition rate was calculated based on three best replicates in the study.

Solution analysis before entering and after exiting the heated cell was made to find out the composition of the scale-forming solution. Ion chromatography was used to determine chlorides and sulfates. Total dissolved solids (TDS) were determined gravimetrically, while the metals were determined by inductively coupled plasma-atomic emission spectroscopy technique.

The surface texture of the 120 and 600 grit polished aluminum samples was determined by using a Bendix Linear Profile System, Model 5054. The measurements were performed at 20 ± 0.5°C and relative humidity of $40 \pm 5\%$. The average roughness of the test samples was measured using linear profiling system which consisted of a console mounted pilotor, a tracer with diamond stylus, a profiling amplifier and a strip chart recorder. The pilotor provided a straight line datum axis and moved the tracer along the surface of a workpiece placed on the surface plate of the console. As the tracer stylus was displaced by the irregularities in the past surface of the sample, electrical signals generated by the tracer were amplified, filtered, and recorded on a strip chart. The surface roughness of the test piece was measured both in forward and reverse direction of the tracer.

An analytical laboratory balance with an accuracy of ±0.1 mg was used to measure the weight gain of scaled specimens after drying in oven. The scale deposition rate was calculated by dividing the weight of scale obtained on per unit area by the duration of the experiment. Data presentation, analyses, plotting, etc., were accomplished by using Microsoft Excel spreadsheet software.

The morphology of calcium sulfate scale crystals was studied by using flat aluminum coupons having dimensions of 20 by 8 by 1.5 mm. The coupons were also polished to 120 and 600 grit with SiC emery papers. After polishing, they were thoroughly degreased with acetone and rinsed with distilled water. Duplicate specimens were assembled in a Teflon holder that was placed in the test cell where they were exposed to the calcium sulfate scale-forming solution for 1–6 h under the same test conditions mentioned above. After the tests, the coupons were retrieved, rinsed with distilled water, dried in an oven and preserved for scanning electron microscopic (SEM) examination to reveal the morphology of the hydrodynamically deposited crystals of $CaSO_4$ on the aluminum substrate.

III. Data Reduction and Experimental Uncertainty

The collected experimental data were subjected to uncertainty analysis. The method for performing the uncertainty analysis for the present experimental investigation has been taken from Taylor and Kuyatt [25]. The procedure adopted for the current uncertainty analysis is summarized as follows:

A. Calculation of Reynolds Number and its Uncertainty

For each preset rotational speed, the equivalent Reynolds numbers Re were computed from the equation suggested by Gabe [14] as follows:

$$Re = f(R_1, R_2, \omega, \nu) \qquad Re = R_1\omega[(R_2 - R_1)/\nu] \tag{1}$$

and

$$(U_{c,Re})^2 = \left(\frac{\partial Re}{\partial R_1}u_{R_1}\right)^2 + \left(\frac{\partial Re}{\partial \omega}u_{\omega}\right)^2 + \left(\frac{\partial Re}{\partial R_2}u_{R_2}\right)^2 + \left(\frac{\partial Re}{\partial \upsilon}u_{\upsilon}\right)^2 \tag{2}$$

The uncertainty propagation for the dependent variable Re, in terms of the measured values has been calculated using the Engineering Equation Solver (EES) software. The measured variables have random variability that is referred to as its uncertainty. Therefore, the uncertainty in Reynolds number ($U_{c,Re}$) in the present study has been found to vary between ±10%. The individual errors contributed to the uncertainty of Reynolds number for the measured or physical properties are: radius of the specimen R_1, ±2%, angular velocity ω, ±3% the radius of the cell R_2, ±2%, and kinematic viscosity, ±3%.

B. Calculation of Scale Deposition Rate and its Uncertainty

As mentioned in the previous section, because the scale deposition rate was calculated by dividing the weight of scale obtained on per unit area by the duration of the experiment, therefore, the data reduction equation is as follows:

$$D_r = f(W_g, R_1, L, t) \qquad D_r = W_g/[(2\pi * R_1 Lt) * 10^4] \tag{3}$$

and

$$(U_{c,Dr})^2 = \left(\frac{\partial D_r}{\partial W_g}u_{w_g}\right)^2 + \left(\frac{\partial D_r}{\partial R_1}u_{R_1}\right)^2 + \left(\frac{\partial D_r}{\partial L}u_L\right)^2 + \left(\frac{\partial D_r}{\partial t}u_t\right)^2 \tag{4}$$

Again the uncertainty propagation for the dependent variable Dr, in terms of the measured values has been calculated using the EES software. Therefore the uncertainty in the deposition rate ($U_{c,Dr}$) in the present study has been found to vary between ±12%. The individual errors contributed to the uncertainty of deposition rate for the measured or physical properties are: weight gained by the specimen W_g, ±6%, radius of the specimen R_1, ±2%, length of the specimen L, ±2%, $\alpha\nu\delta$ time-duration of the experiment t, ±2%.

IV. Results and Discussion

A. Surface Roughness

The average surface roughness Ra values for 600 and 120 grit polished samples measured were 82.5 μ-in. (2.0955 μ m) and 120 μ-in. (3.048 μ m). The low value of Ra indicates a smooth surface texture, while the high value shows a rough surface profile. The 600 grit polishing thus rendered a smooth surface, whereas 120 grit polishing produced comparatively a coarse surface finish.

B. Induction Period

The induction period obtained in the study for the 120 grit polished samples was 40 ± 2 min while for 600 grit polished samples, it was 50 ± 2 min at 60°C. Similarly at 70°C, the induction time was found to be 30 ± 2 min for 120 grit polished samples, while it was 35 ± 2 min for 600 grit polished samples. At 70°C temperature the induction period obtained is less compared with at 60°C; this is because of the inverse solubility effect of the scaling solution. Therefore, at higher temperatures and/or higher concentration of dissolved inorganic salts, spontaneous (heterogeneous) bulk precipitation of the scaling solution occurs, which reduces the induction period [23], and under such conditions induction period can sometimes even approach to zero.

C. Solution Composition

The composition of the scale-forming solution determined by the techniques described in the experimental section, at the inlet and exit from the test cell is given in the Table 1. After inspection, almost constant composition of the scale-forming solution can be seen from the table, at the inlet and outlet of the test cell. The analyses therefore show that the samples were exposed to a uniform composition of the scale-forming solution throughout the experiments duration. The concentration of the ionic species present in the solution used in our study is low as compared with solutions used in other research studies [20,21].

Based on our prior experience (beaker tests), we chose low concentration of salts so that no precipitation could occur at room temperature after commingling of two solutions for at least 8–10 h in the reservoir and, therefore, the whole chemical reaction (i.e., precipitation) must occur upon heating the solution in the glass test cell. This was, also, our ultimate manifestation in the present work. On the contrary, if the concentration of the dissolved mineral salts is higher then the precipitation can occur spontaneously at room temperature upon mixing of the two solutions due to enhanced supersaturation. The higher temperature on the other hand also leads to instant precipitation. Therefore, the precipitation is dependent on

Table 1 Chemical analysis of the $CaSO_4$ scaling solution at inlet and after exit from the test cell

Sampling position	Composition (ppm or mg/L)							
	Ca^{2+}	Na^{+}	Mg^{2+}	Cl^{-}	SO_4^{2-}	pH	Total hardness	TDS
At inlet	1010	1150	0.202	2150	2040	5.55	2520	6400
At exit	1020	1150	0.228	2140	2210	5.84	2550	6800

the degree of supersaturation of the scale-forming solution, as well as it is temperature sensitive [23].

D. Scale Deposition

The speed of rotation of the specimen as well as mixing of solution had a strong influence on the rate of mass transport of $CaSO_4$ scale to the electrode surface where it was adsorbed and eventually deposited on the surface of the specimens at the selected temperatures and at various rotational speeds, which yielded measurable weight gain of scale on the aluminum samples.

Analysis of the data was carried out to demonstrate the effect of solution hydrodynamics on the deposition rate. For this, various Reynolds numbers were obtained and tested corresponding to each selected rotational speed as suggested by Gabe [14]. It is to be noted that normally, the RCE and RDE systems generate turbulence when RPM $\geq$ 200 [14]. Therefore, we conducted our study in the turbulent regime (from 250 to 2000 RPM, i.e., corresponding to equivalent Reynolds number of 3642 to 29135 [14]).

The average scale deposition rate versus Reynolds numbers are plotted in Fig. 2 to show the effect of calcium sulfate scale deposition on 120 and 600 grit polished aluminum samples at temperatures of 60 and 70°C, respectively. The results show an increasing trend in the data obtained and are in agreement with the earlier studies [8,9,17,18].

Figure 2 further delineates the effect of surface finish of aluminum samples produced with 120 and 600 grit SiC emery papers. The 600 grit polished samples showed more weight gain than 120 grit samples.

An increasing trend can be observed from Fig. 2, for scale deposition at 70°C. The figure further shows the deposition rate for 600 grit polished samples at the two selected temperatures of 60 and 70°C. At 70°C, the rate of scale deposition increased significantly as compared with 60°C for 600 grit polished aluminum samples. A high rate of precipitation is expected at increased temperature because of inverse solubility characteristics of the scale-forming solution. Thus, due to the inverse solubility effect of the supersaturated solution, more precipitation is always expected at higher temperatures. This phenomenon is actually attributable to the chemistry behind the precipitation scaling/fouling resulting from the supersaturated scaling solution (upon heating) and the subsequent deposition of scale on the metal surface (physics).

In our experimental study, we kept the solution's ionic chemistry constant by replenishment of fresh solution to the test cell and varied other parameters of interest, that is; temperature, surface roughness and rotational speed to understand the mechanism of scale formation and its deposition on aluminum surface. Scaling is a complex process nevertheless the following paragraphs provide an overall explanation of the scale deposition process on the surface of the specimen in a relatively simple way.

The chemical equation governing the precipitation of scaling species due to the double displacement chemical reaction resulting from the mixing of two equimolar solutions upon heating in the test cell at the selected temperature is given in Eq. (5), as follows:

$$Na_2SO_4(aq) + CaCl_2(aq) \rightarrow CaSO_4(s) + 2NaCl(aq) \quad (5a)$$

The reactants are ionic compounds, therefore, the above equation can be written in ionic form as:

$$Ca^{2+} + SO_4^{2-} \rightarrow CaSO_4(s) \quad (5b)$$

Because of chemisorption of calcium cations (Ca^{2+}) and sulfate anions (SO_4^{2-}), $CaSO_4$ is precipitated as solid phase gypsum [Eq. (5)]. These tiny precipitating particles (called nuclei) of $CaSO_4$ in the bulk of the scaling solution after gaining weight due to coalescence deposit on the active nucleation sites present on the surface of the specimens. So the nucleation process is multifaceted during the scale deposition process. First nucleation is occurring in the bulk of the scaling solution due to chemical reaction [Eq. (5)]. This nucleation can be homogeneous or heterogeneous (spontaneous scale/crystals growth), which ultimately results in the precipitation of the $CaSO_4$ particles in the bulk of the solution. Whilst, the second nucleation takes place on the surface of the specimen at active nucleation sites which are the result of surface heterogeneities (irregularities) present due to kinks, ledges, screw-dislocations, scratches, polishing marks, etc., that eventually attract the precipitating scaling species toward them (diffusion) and finally these particles adhere at these sites on the surface of metal due to mechanical bonding (physics) which finally results in scale growth and deposition on the metal surface.

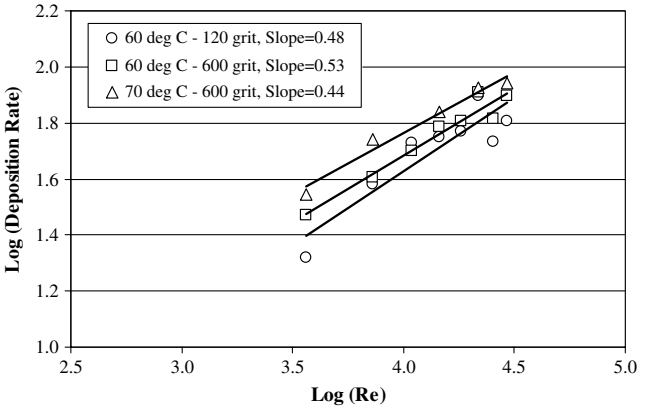

Fig. 2 Average deposition rate of calcium sulfate scale on 120 and 600 grit polished aluminum surface as a function of Reynolds number at 60 and 70°C.

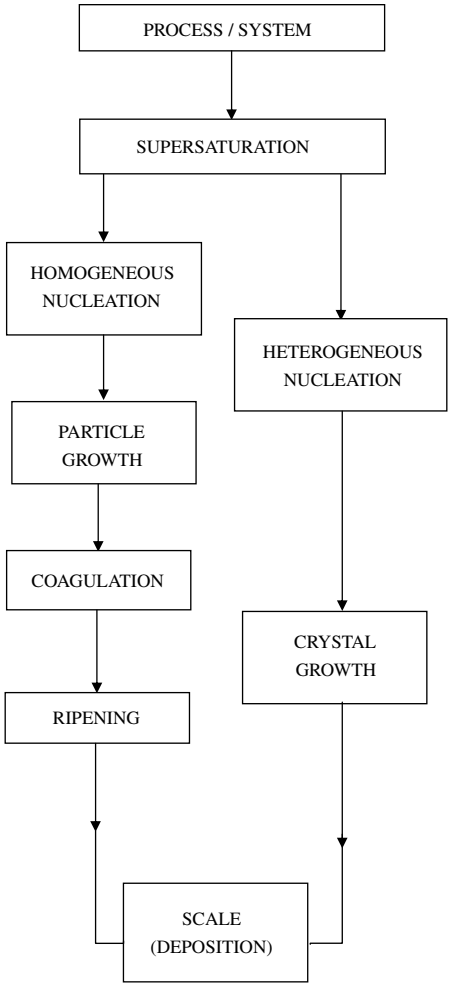

Fig. 3 Schematic representation of the scale deposition mechanism from process/system on the metal surface.

A simplified schematic representation of the scale deposition mechanism resulting from the process fluid stream or any such incompatible cooling water system is shown in Fig. 3. The figure shows two important crystallization paths; 1) homogeneous crystallization, and 2) heterogeneous crystallization. When there is a single precipitating salt with low concentration and moderate temperature without any external contamination, the crystallization process results as homogeneous. Conversely, if the concentration and temperature are higher or with presence of external seeding and impurities (suspended solids, biomass), or there are multi salts with high concentrations present in the solution, the process leads to heterogeneous (instant) crystallization. It is to be noted that the localized hot spots or burnouts or collapsing of bubbles on the surface will also result in heterogeneous precipitation. We used low concentrations and moderate temperature to deposit single pure salt ($CaSO_4$), which followed the homogeneous crystallization process in our experimental study.

The above behavior indicates that the precipitation (chemistry) and the adhesion/anchorage (physics) of scale to the substrate surface are different mechanisms. The precipitation is occurring due to the chemical potential (ionic strength) which is provided by the supersaturation of the solution (constant in our case) while the adhesion on the metal surface mainly depends on the diffusion (transport of mass/scale particles) to the surface and the adsorption of scaling *adions* on the surface and then finally the incorporation of these adions into the surface lattice of metal which is provided by the surface binding energy of the metal at the active nucleation sites. These surface heterogeneities are mainly considered low energy sites, so the physics plays an important role in the adhesion of scale onto the surface of metal.

In our experimental study though, the chemical reaction was continuously producing precipitation in the bulk of the solution [Eq. (5)] due to the replenishment of the fresh solution. However, at high rotational speeds, tangential forces or shear stresses increase too, so the scale removal process at the solid–liquid interface may become significant along with the scale deposition process. Secondly, the residence or contact time for the scale to remain attached to the surface of specimens becomes less and thirdly, possibly the affinity (due to surface binding energy, surface tension or wetness of the metal) towards scale is not strong. This may be the reason that the rate of scale deposition comparatively falls off to some extent at higher rotational speeds.

Thus, in certain cases, the turbulence generated due to high rotational speeds (flow velocity) may be advantageous to some extent as a mean of scale removal due to high shear stresses depending on the nature of scale (e.g., $CaSO_4$), as it may wash away the freshly depositing layers of scale on the previously deposited scale or may break and carry away flake/chunk of already deposited crystals (i.e., reverse process under favorable conditions due to high velocity). However, for other types of scales it is equally likely that it may not be effective over the periods of time relevant in the industrial context. For example, complete choking of oil production tubing strings have been observed in the Gulf region, as Singh and Abbas [24] conducted their analysis on scale samples removed from choked oil production tubings.

Some tiny flakes of scale were seen floating in the glass cell at high rotational speeds ($\geq$ 1500 rpm), which could be attributed to relatively poor adhesion of scale onto the substrate or breaking away of some portion of previously deposited scale during the scale removal process. Another reason could be that since the $CaSO_4$ crystals growth is of needle-type (see morphology section) they may break away due to high velocity. This may be the reason for the disparity in the data for the 600 grit polished samples shown in Fig. 2 at higher rotations. Therefore, in scaling/fouling process both the scale deposition and scale removal occur and compete each other simultaneously, however, the dominant process (deposition or removal) will take over the precedence and show its effect with the passage of time., and the behavior may change with time (linearly increasing, falling rate, asymptotic or saw tooth rate [26]).

The above mentioned growth and dissolution mechanism from the incompatible waters or supersaturated solutions can therefore be briefly summarized in the following steps: 1) precipitation due to supersaturation, 2) diffusion of solutes/scaling species to the surface, 3) adsorption onto the surface to form adions, 4) incorporation of the adions into the surface lattice, and 5) reverse sequence for dissolution if the conditions are correct and favorable.

Plotted in Fig. 4 is a comparison between the deposition rate of $CaSO_4$ scale on aluminum and stainless steel-316 [18], under identical experimental conditions. The figure shows that the $CaSO_4$ scale deposition is more on aluminum compared with stainless steel-316. Because every material has its own pertinent characteristics such as surface activation energy and/or surface wetness/wetability, therefore, it seems that the conditions for deposition on aluminum were more favorable compared with stainless steel. However, we observed that the deposition on aluminum was fluffy at lower speed, nonuniform especially at higher rotations and not strongly adhering to the surface, whereas, it was uniform and strongly adhering to the surface of SS-316 [18].

It is to be noted that during scale formation process on the surface of metal, once an initial thin layer of scale is formed on the surface the subsequent scale growth on it is much faster because of readily available abundant nucleation sites as compared with a polished surface. Also, the scaled surface provides larger surface area, which promotes deposition process compared with a bare or polished surface. The existing layers of scale provide more nucleation sites for the subsequent scale growth and anchorage, which promote scale deposition process.

The present results in the study were obtained by using pure salts without any seeding or contamination. The seeding is normally used to quicken crystallization process [4]. However, the presence of impurities such as particulates, suspended solids, mixed salts, corrosion products, biological matters, surface geometry and flow velocity, etc., have significant impact on the deposition behavior of scale on the surface. The conjoint effect of all these impurities may affect the overall growth rate of scale. Therefore, under such circumstances, the scaling or fouling rate may result in linear (increasing or falling) or asymptotic [26,27] rates. The asymptotic behavior in scaling or fouling of heat exchange equipment is observed when the rate of deposition of scale is balanced by the rate of removal of scale under process fluid flow conditions.

E. Diffusional Mass Transport

The data presented in Figs. 2 shows that the $CaSO_4$ scaling rate increases with Reynolds number suggesting further that the process is mass transport dependent. According to Levich [28], the mass transfer coefficient should increase with $(Re)^{0.5}$. If so, the plot of {log(deposition)} verses {log(Re)} should give a straight line with a theoretical slope of 0.5.

Figure 2 also shows the diffusional mass transport effect for the data generated in the study for 60 and 70°C, respectively. A straight line behavior is depicted from the figure with slopes of 0.48 for 120 grit surface polish and 0.53 for 600 surface polish at 60°C, and 0.44

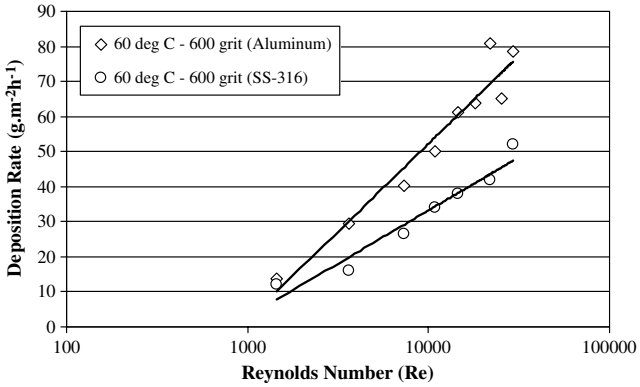

Fig. 4 Comparison of average deposition rate of calcium sulfate scale on aluminum and SS-316 [18].

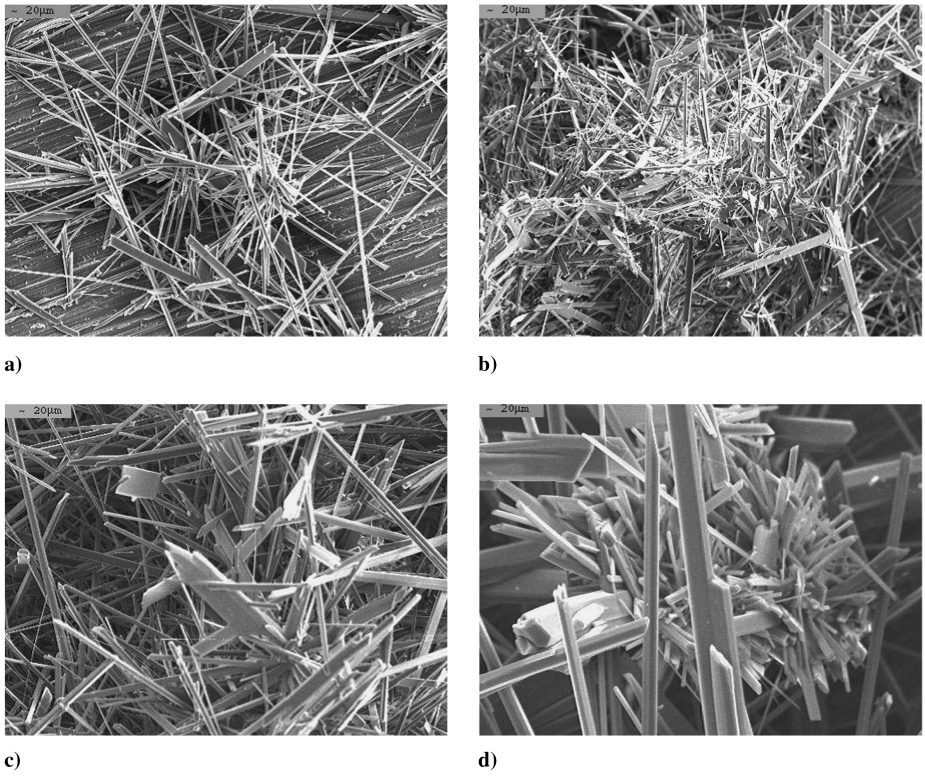

Fig. 5 SEM micrographs showing morphology of $CaSO_4$ crystals on aluminum substrate: a) needles: after 2 h, b) needles: after 4 h, c and d) needles, flat crystals, prismatic rod, secondary and perpendicular growth: after 6 h.

for 600 grit polish samples at 70°C. The slopes were determined from the best fit of straight lines in the data developed using Excel spreadsheet program. The slopes of the best-fitted lines are close to the theoretically predicted value of 0.5. Therefore, the results of the study demonstrate the diffusion controlled (mass transport) aspect of the scale deposition process.

F. Morphology

The scanning electron microscopy examination of the $CaSO_4$ scale exhibited crystal structures consisting of mainly monoclinic or prismatic needle- and/or rodlike growth. However, at certain locations some flat crystals were also evident, which had been formed due to the coagulation of prismatic needles/rods. In general, the growth of $CaSO_4$ (gypsum) crystals initially started at the active nucleation sites on the substrate surface or on the existing crystals and then apparently branched out randomly in all directions. We used pure salts to prepare scale-forming solution, therefore energy dispersive *X* ray diffraction spectroscopy showed high peaks for calcium and sulfur rich crystals, which ratified that these were of $CaSO_4$ scale.

As revealed by the SEM examination, Fig. 5 presents some typical results of the morphology of calcium sulfate crystals deposited on aluminum substrate after 2, 4, and 6 h of exposure to the scale-forming solution. At the beginning, few scale crystals initially grew in the shape of tiny prisms, which developed further into needles (Fig. 5a), or prismatic rods and then as the exposure time increased, these needles conglomerated to form thick rods or flat crystals. The photomicrographs in Fig. 5b show the presence of a dense population of uniformly distributed $CaSO_4$ crystals on the entire surface of the aluminum substrate. Similar results were obtained in earlier studies for the $SrSO_4$ [5], $BaSO_4$ [17] and $CaSO_4$ [18] scale formation on stainless steel 316. The micrographs shown in Figs. 5c and 5d, however, further indicate the apparently random growth of subsequent crystals emanating from the already deposited primary crystals. In addition, the secondary as well as perpendicular growth of $CaSO_4$ crystals is also evident in these micrographs. The crystals thus, seem to have been growing at preferential nucleation sites available on the substrate and/or on the previously deposited scale layer.

V. Conclusions

The ionic chemistry of the scaling solution was kept constant by continuous replenishment of the fresh solution to the test cell and varied other parameters such as temperature, surface roughness, and rotational speeds to discern their effects on scale formation process. The following are the main concluding points of the study:

1) The solution hydrodynamics plays a significant role in the scale deposition process. The turbulent mixing generated due to the agitation of the solution promoted scale formation by allowing more active scale-forming species to adsorb on the metal surface, which subsequently adhered and deposited on the substrate. Therefore, the hydrodynamic factor is important and must be taken into consideration while developing any scale control strategy or scale prediction model.

2) The 600 grit polished surface showed more deposition compared with 120 grit polished surface and the deposition rate of calcium sulfate scale on aluminum was significantly higher as compared with stainless steel 316 under identical test conditions.

3) The increase in temperature has a significant effect on scale deposition because of the inverse solubility effect of the supersaturated scaling solution. Therefore, at higher temperature of 70°C more deposition of calcium sulfate scale on aluminum was observed than at 60°C at the same surface roughness conditions.

4) The scale deposition rate versus Reynolds number showed an increasing trend for the data developed in the present work; however, in practical industrial situations, the deposition may possibly show a different behavior, e.g., falling rate or asymptotic. In addition, the scale deposition data presented supports mass transport (diffusion) process.

5) The SEM examination revealed crystal structures on microscopic level as monoclinic, prismatic needles, rods, and flat crystals. Generally, the growth of $CaSO_4$ crystals initially started at the nucleation sites available on the aluminum surface and then branched out apparently randomly in all directions as the exposure

continued. Secondary crystals growth of scale on the primary crystals was also observed from SEM imagery.

Acknowledgments

The support of the Ministry of Higher Education and the Research Institute of King Fahd University of Petroleum and Minerals for this work is highly acknowledged.

References

[1] Potts, D. E., Ahlert, R. C., and Wang, S. S., "A Critical Review of Fouling of Reverse Osmosis Membranes," *Desalination*, Vol. 36, No. 3, 1981, pp. 235–264. doi:10.1016/S0011-9164(00)88642-7

[2] Cowan, J. C., and Weintritt, D. J., *Water Formed Scale Deposits*, Gulf Publishing Co., Houston, Texas, 1976.

[3] Al-Ahmed, M., and Aleem, F. A., "Scale Formation and Fouling Problems Effect on the Performance of MSF and RO Desalination Plants in Saudi Arabia," *Desalination*, Vol. 93, Nos. 1–3, 1993, pp. 287–310. doi:10.1016/0011-9164(93)80110-9

[4] Sung–Tsuen, L., and Nancollas, G. H., "The Kinetics of Crystal Growth of Calcium Sulfate Dihydrate," *Journal of Crystal Growth*, Vol. 6, No. 3, 1970, pp. 281–289. doi:10.1016/0022-0248(70)90081-3

[5] Khokhar, M. I., Somuah, S. K., Amabeoku, M. O., Allam, I. M., and Quddus, A., "Oilfield Scaling: Mechanism of Formation," *Proceeding of the 4th Middle East Corrosion Conference, Bahrain*, Part 1, 1988, pp. 244–258.

[6] Zubair, S. M., Sheikh, A. K., Budair, M. O., Haq, M. U., Quddus, A., and Ashiru, O. A., "Statistical Aspects of $CaCO_3$ Fouling in AISI 316 Stainless Steel Tubes," *Journal of Heat Transfer*, Vol. 119, No. 3, 1997, pp. 581–588. doi:10.1115/1.2824145

[7] Budair, M. O., sultan, M. S., Zubair, S. M., Sheikh, A. K., and Quddus, A., "$CaCO_3$ Scaling in AISI 316 Tubes—Effect of Thermal and Hydraulic Parameters on the Induction Time and Growth Rate," *Journal of Heat Transfer*, Vol. 34, 1998, pp. 163–170.

[8] Hasson, D., Avriel, M., Resnick, W., Rosenman, T., and Windreich, S., "Mechanism of Calcium Carbonate Scale Deposition on Heat-Transfer Surfaces," *Industrial and Engineering Chemistry Fundamentals*, Vol. 7, No. 1, 1968, pp. 59–65. doi:10.1021/i160025a011

[9] Hasson, D., and Zahavi, J., "Mechanism of $CaSO_4$ Scale Deposition on Heat Transfer Surfaces," *Industrial and Engineering Chemistry Fundamentals*, Vol. 9, No. 1, 1970, pp. 1–10. doi:10.1021/i160033a001

[10] Liu, G., Tree, D. A., and High, M. S., "Relationship Between Rotating Disk Corrosion Measurements and Corrosion in Pipe Flow," *Corrosion*, Vol. 50, No. 8, 1994, pp. 584–593. doi:10.5006/1.3293529

[11] Efrid, K. D., Wright, E. J., Boros, J. A., and Hailey, T. G., "Correlation of Steel Corrosion in Pipe Flow with Jet Impingement and Rotating Cylinder Tests," *Corrosion*, Vol. 49, No. 12, 1993, pp. 992–1003. doi:10.5006/1.3316026

[12] Silverman, D. C., "Rotating Cylinder Electrode for Velocity Sensitivity Testing," *Corrosion*, Vol. 40, 1984, pp. 220–226.

[13] Silverman, D. C., "Rotating Cylinder Electrode: Geometry Relationships for Prediction of Velocity-Sensitive Corrosion," *Corrosion*, Vol. 44, 1988, pp. 42–49.

[14] Gabe, D. R., "The Rotating Cylinder Electrode," *Journal of the Electrochemical Society*, Vol. 4, 1974, pp. 91–108.

[15] Ashiru, O. A., and Farr, J. P. G., "Kinetics of Reduction of Silver Complexes at the Rotating Disk Electrode," *Journal of the Electrochemical Society*, Vol. 139, No. 10, 1992, pp. 2806–2810. doi:10.1149/1.2068983

[16] Low, C. T. J., de Leon, C. P., and Walsh, F. C., "The Rotating Cylinder Electrode (RCE) and its Application to the Electrodeposition of Metals," *Australian Journal of Chemistry*, Vol. 58, No. 4, 2005, pp. 246–262. doi:10.1071/CH05034

[17] Quddus, A., and Allam, I. M., "$BaSO_4$ Scale Deposition on Stainless Steel," *Desalination*, Vol. 127, 2000, pp. 127–131.

[18] Quddus, A., "Effect of Hydrodynamics on the Deposition of $CaSO_4$ Scale on Stainless Steel," *Desalination*, Vol. 142, No. 1, 2002, pp. 57–63. doi:10.1016/S0011-9164(01)00425-8

[19] Neville, A., Morizot, A. P., and Hodgkiess, T., "Electrochemical Aspects of Surface/Solution Interactions on Scale Initiation and Growth," *Materials Performance*, Vol. 37, No. 5, 1998, pp. 50–57.

[20] Neville, A., Morizot, A. P., and Hodgkiess, T., "Electrochemical Assessment of $CaCO_3$ Deposition Using a Rotating Disc Electrode," *Journal of Applied Electrochemistry*, Vol. 29, No. 4, 1999, pp. 455–462. doi:10.1023/A:1026431519148

[21] Neville, A., Morizot, A. P., "Calcareous Scale Formed by Cathodic Protection—An Assessment of Characteristics and Kinetics," *Journal of Crystal Growth*, Vol. 243, Nos. 3–4, 2002, pp. 490–502. doi:10.1016/S0022-0248(02)01532-4

[22] Morizot, A., Neville, A., and Hodgkiess, T., "Studies of Deposition of $CaCO_3$ on a Stainless Steel Surface by a Novel Electrochemical Technique," *Journal of Crystal Growth*, Vol. 198–199, 1999, pp. 738–743. doi:10.1016/S0022-0248(98)01035-5

[23] Chen, T., Neville, A., and Yuan, M., "Calcium Carbonate Scale Formation: Assessing the Initial Stages of Precipitation and Deposition," *Journal of Petroleum Science and Engineering*, Vol. 46, No. 3, 2005, pp. 185–194. doi:10.1016/j.petrol.2004.12.004

[24] Singh, R. P., and Abbas, N. M., "Characterization of Oilfield Scales," *Proceedings of the 5th Middle East Corrosion Conference, Bahrain*, Vol. 4, 1991, pp. 561–569.

[25] Taylor, B. N., and Kuyatt, C. E., "Guidelines for Evaluating and Expressing the Uncertainty of NIST Measurement Results," National Institute of Standards and Technology, Gaithersburg, MD, 1994, p. 1297.

[26] Knudsen, J. G., "Cooling Water Fouling: A Brief Review," *Proceeding of the 20th ASME/AIChE Heat Transfer Conference*, Vol. 17, American Society of Mechanical Engineers, Fairfield, NJ, 1981, pp. 29–38.

[27] Hewitt, G. F., *Hemisphere Handbook of Heat Exchanger Design*, Section 3.17, Hemisphere Publishing Corporation, New York, 1990.

[28] Levich, V. G., *Physicochemical Hydrodynamics*, Prentice–Hall, Englewood Cliff, NJ, 1962.